

# Apolipoprotein CIII Overexpressing Mice Are Predisposed to Diet-Induced Hepatic Steatosis and Hepatic Insulin Resistance

Hui-Young Lee,<sup>1,2,3</sup> Andreas L. Birkenfeld,<sup>1</sup> Francois R. Jornayvaz,<sup>1</sup> Michael J. Jurczak,<sup>1,3</sup> Shoichi Kanda,<sup>1</sup> Violeta Popov,<sup>1</sup> David W. Frederick,<sup>1</sup> Dongyan Zhang,<sup>1,3</sup> Blas Guigni,<sup>1</sup> Kalyani G. Bharadwaj,<sup>4</sup> Cheol Soo Choi,<sup>1</sup> Ira J. Goldberg,<sup>4</sup> Jae-Hak Park,<sup>5</sup> Kitt F. Petersen,<sup>1,2</sup> Varman T. Samuel,<sup>1,2</sup> and Gerald I. Shulman<sup>1,2,3</sup>

**Nonalcoholic fatty liver disease (NAFLD) and insulin resistance have recently been found to be associated with increased plasma concentrations of apolipoprotein CIII (APOC3) in humans carrying single nucleotide polymorphisms within the insulin response element of the APOC3 gene. To examine whether increased expression of APOC3 would predispose mice to NAFLD and hepatic insulin resistance, human APOC3 overexpressing (ApoC3Tg) mice were metabolically phenotyped following either a regular chow or high-fat diet (HFD). After HFD feeding, ApoC3Tg mice had increased hepatic triglyceride accumulation, which was associated with cellular ballooning and inflammatory changes. ApoC3Tg mice also manifested severe hepatic insulin resistance assessed by a hyperinsulinemic-euglycemic clamp, which could mostly be attributed to increased hepatic diacylglycerol content, protein kinase C- $\epsilon$  activation, and decreased insulin-stimulated Akt2 activity. Increased hepatic triglyceride content in the HFD-fed ApoC3Tg mice could be attributed to a  $\approx$ 70% increase in hepatic triglyceride uptake and  $\approx$ 50% reduction hepatic triglyceride secretion. **Conclusion:** These data demonstrate that increase plasma APOC3 concentrations predispose mice to diet-induced NAFLD and hepatic insulin resistance. (HEPATOLOGY 2011;54:1650-1660)**

**H**epatic insulin resistance associated with non-alcoholic fatty liver disease (NAFLD) is a major factor contributing to the pathogenesis of type 2 diabetes.<sup>1-3</sup> Hepatic fat accumulation is the result of an imbalance between lipid delivery and *de novo* lipogenesis and lipid disposal either by oxidation or export in very low density lipoproteins (VLDL). Apolipoprotein CIII (APOC3) has been shown to be an important factor in regulating plasma triglyceride concentrations; in both rodents and human subjects increased expression of APOC3 is associated with

higher plasma triglyceride levels and a null mutation with reduced triglyceride levels.<sup>4,5</sup> APOC3 predominantly affects VLDL-triglyceride metabolism and greater APOC3 production can increase VLDL-triglyceride production and reduce hepatic clearance of triglyceride rich lipoproteins (TGRLs).<sup>6</sup> APOC3 stimulates VLDL synthesis and secretion in cultured hepatocytes<sup>7</sup> and elevated circulating APOC3 levels correlate with VLDL production<sup>8</sup> and higher postprandial hyperlipidemia in humans.<sup>9</sup> Furthermore, APOC3 expression was proinflammatory in endothelial

*Abbreviations: apoB, apolipoprotein B; APOC3, apolipoprotein CIII; ApoC3Tg, transgenic mice with hepatic overexpression of human APOC3; APOE, apolipoprotein E; AUC, area under curve; CM, chylomicron; DAG, diacylglycerol; EGP, endogenous glucose production; HFD, high-fat diet; IPGTT, intraperitoneal glucose tolerance test; JNK, c-Jun N-terminal kinase; LpL, lipoprotein lipase; MTP, microsomal triglyceride transfer protein; NAFLD, nonalcoholic fatty liver disease; NASH, nonalcoholic steatohepatitis; NAS, NAFLD activity score; NF- $\kappa$ B, nuclear factor kappaB; PKC $\epsilon$ , protein kinase C- $\epsilon$ ; PPAR- $\alpha$ , peroxisome proliferator-activated receptor; RC, regular chow; RE, retinyl ester; SREBP-1c, sterol regulatory element binding protein-1c; TGRLs, triglyceride rich lipoproteins; TNF- $\alpha$ , tumor necrosis factor-alpha; VLDL, very low density lipoproteins; WT, wildtype littermates.*

*From the <sup>1</sup>Department of Internal Medicine, Yale University School of Medicine, New Haven, CT; <sup>2</sup>Department of Cellular & Molecular Physiology, Yale University School of Medicine, New Haven, CT; <sup>3</sup>Howard Hughes Medical Institute, Yale University School of Medicine, New Haven, CT; <sup>4</sup>Department of Medicine, Columbia University, New York, NY; and <sup>5</sup>Department of Laboratory Animal Medicine, College of Veterinary Medicine, Seoul National University, Seoul, Korea.*

*Received April 25, 2011; accepted July 12, 2011.*

*Supported by grants from the United States Public Health Service (R01 DK-40936, R01 AG-23686, R24 DK-085638, U24 DK-059635, HL-45095), German Research Association Bi1292/2-1 (to A.B.) and Swiss National Science Foundation/Swiss Foundation PASMP3-132563 (to F.J.).*

*K.P. is the recipient of a Distinguished Clinical Investigator Award from the American Diabetes Association.*

cells<sup>10</sup> and adipose tissue.<sup>11</sup> Elevated circulating APOC3 levels are associated with many diseases including metabolic syndrome,<sup>12</sup> coronary artery disease,<sup>5</sup> and insulin resistance<sup>9,13</sup> both in humans and animal models.

Recently, we found that common rs2854116 [T-455C] and rs2854117 [C-482T] single nucleotide polymorphisms in an insulin-response element of the promoter region in the APOC3 gene were associated with increased plasma APOC3 concentrations and an increased prevalence of NAFLD and whole-body insulin resistance in healthy lean men.<sup>9</sup> These results suggest that increased plasma APOC3 concentrations may predispose lean individuals to NAFLD and hepatic insulin resistance, although the underlying mechanisms for hepatic lipid accumulation and insulin resistance are unclear.

In order to examine these questions we examined: (1) whether transgenic mice with hepatic overexpression of human APOC3 (ApoC3Tg) are prone to develop nonalcoholic steatohepatitis (NASH); (2) whether NAFLD is associated with hepatic insulin resistance in this model; (3) the underlying mechanism by which these mice develop NAFLD; and (4) the cellular mechanisms by which NAFLD in these mice leads to hepatic insulin resistance.

## Materials and Methods

**Animals.** The ApoC3Tg mice, under the control of its native promoter in the C57BL/6J background,<sup>4,6</sup> were further backcrossed with female C57BL/6J mice over five generations in the Yale animal facility. Male ApoC3Tg mice and age-matched littermate control male mice (WT) were studied at the age of 4 to 8 months. Mice were individually housed under controlled temperature (23°C) and lighting (12/12-hour light/dark) with free access to water and fed ad libitum on regular chow (RC, 2018S, Harlan Teklad) and a high-fat diet (HFD, 55% calories from fat, TD93075, Harlan Teklad). Body composition was assessed by <sup>1</sup>H magnetic resonance spectroscopy (Bruker BioSpin). Whole-body energy metabolism including VO<sub>2</sub>, VCO<sub>2</sub>, energy expenditure, locomotor activity, and food intake were measured for 72 hours by indirect calorimeter (CLAMS, Columbus Instrument). The study was conducted at the NIH-Yale Mouse Meta-

bolic Phenotyping Center. All procedures were approved by the Yale University Animal Care and Use Committee.

**Plasma Parameters.** Blood samples were taken from the tail vein after an overnight fast. Plasma triglyceride and nonesterified fatty acid concentrations were determined using standard commercial kits according to the manufacturer's instructions (Diagnostic Chemicals and Wako Chemicals, respectively). Plasma insulin and adiponectin levels were measured by radioimmunoassays (Linco, Billerica, MA). Plasma glucose was measured with a glucose analyzer (Beckman Coulter, Brea, CA). Human APOC3 concentrations were measured with Cobas Mira plus (Roche Diagnostic, Indianapolis, IN). Mouse cytokine array (RayBio) was conducted as described in the manufacturer's description.

**Liver Histology.** Liver sections for histology were obtained after overnight fasting, fixed in 10% formalin, and stained with hematoxylin-eosin or Masson trichrome. Histology was read by two independent pathologists blinded to experimental design and treatment groups. Briefly, steatosis (0-3), lobular inflammation (0-3), ballooning (0-3), and fibrosis (0-4) were scored separately on a scale of 0-4 as described.<sup>14,15</sup> NAFLD activity score is expressed as the sum of each scoring.<sup>15</sup>

**Hyperinsulinemic-Euglycemic Clamp Study.** The mice were maintained on an HFD for ≈2 months. After an overnight fast, [<sup>3</sup>H]-glucose (high-performance liquid chromatography [HPLC] purified; PerkinElmer, Waltham, MA) was infused at a rate of 0.05 μCi/min for 2 hours to assess a rate of basal glucose turnover, followed by a 140-minute hyperinsulinemic-euglycemic clamp with a primed/continuous infusion of human insulin (31.5 mU/kg prime for 3 minutes, 4.5 mU/(kg·min) infusion; Novo Nordisk, Copenhagen, DK) as described.<sup>16,17</sup> Rates of basal and insulin-stimulated whole-body glucose fluxes and tissue glucose uptake were determined by bolus injection of 10 μCi of 2-deoxy-D-[1-<sup>14</sup>C] glucose (PerkinElmer).

**Tissue Lipid Measurements.** Tissue triglyceride was extracted using the method of Bligh and Dyer<sup>18</sup> and measured using a DCL Triglyceride Reagent (Diagnostic Chemicals). Hepatic ceramide species and hepatic cytosolic DAG species were measured after overnight fasting using liquid chromatography and tandem mass

Address reprint requests to: Gerald I. Shulman, M.D., Ph.D., Yale University School of Medicine, TAC S269, P.O. Box 9812, New Haven, CT 06536-8012.  
E-mail: gerald.shulman@yale.edu; fax: 203-737-4059

Copyright © 2011 by the American Association for the Study of Liver Diseases.

View this article online at wileyonlinelibrary.com.

DOI 10.1002/hep.24571

Additional Supporting Information may be found in the online version of this article.

Potential conflict of interest: Dr. Goldberg received grants from A & Z Pharmaceutical. She is a consultant from and is on the speakers' bureau of Merck.

spectrometry as described.<sup>19</sup> Total DAG and ceramide are expressed as the sum of individual species.

**Membrane Translocation of Protein Kinase C- $\epsilon$  (PKC $\epsilon$ ) and Phosphorylated AKT.** PKC $\epsilon$  membrane translocation in the liver protein extracts after overnight fasting and insulin phosphorylation of AKT<sup>Ser473</sup> were assessed both after overnight fasting and after the hyperinsulinemic euglycemic clamp study using the methods described.<sup>20,21</sup> Images were analyzed and quantified with ImageJ (NIH). Membrane translocation of PKC $\epsilon$  was expressed as the ratio of membrane to cytosol bands.

**Tissue Lipid Clearance and Uptake.** Plasma lipid clearance and tissue uptake were assessed using mouse [<sup>3</sup>H]-labeled triolein and endogenously dual labeled chylomicrons (CM), including [<sup>3</sup>H]-retinyl ester and [<sup>14</sup>C]-triglyceride. Animals fed HFD for  $\approx$ 3 months were cannulated (jugular vein) 7 days before the injection day. After collection of overnight fasting blood samples, a bolus injection of Liposyn (20%, 0.75 mL/kg, Abbott Laboratories, North Chicago, IL) conjugated with 10  $\mu$ Ci of [9,10-<sup>3</sup>H(N)]-triolein was administered over 1 minute through the jugular vein. Blood samples were collected at 2.5, 5, 7.5, 10, 15, 20, 30, and 60 minutes from tail vein. Endogenously dual-radiolabeled CM were prepared as described.<sup>22</sup> After collection of blood at 0 minutes,  $2 \times 10^5$  dpm of [<sup>14</sup>C]-triglyceride-CM and  $6 \times 10^5$  dpm of [<sup>3</sup>H]-RE-CM were injected. Blood was collected at 2.5, 5, 10, and 15 minutes after injection. Tissue and plasma organic phase were extracted using the method of Bligh and Dyer<sup>18</sup> and <sup>3</sup>H/<sup>14</sup>C radioactivity was measured by beta-counter and the plasma and tissue triglyceride concentration was determined using a DCL Triglyceride Reagent (Diagnostic Chemicals). Tissue-specific triglyceride uptake rates [mg/(kg tissue-min)] were calculated by the following equation: Triglyceride uptake rate [mg/(kg tissue-min)] = plasma triglyceride (mg/ml)  $\times$  {tissue radio-activity [dpm/(kg tissue-min)]/area under curve (AUC) of plasma radioactivity (dpm/ml)}.

**Liver Triglyceride Production.** Mice were maintained on RC or HFD for 3 months. After an overnight fast, plasma triglyceride levels were assayed prior to (0 hours) and 1, 2, 3, and 4 hours after poloxamer407 injection using an enzymatic method (Diagnostic Chemicals). The VLDL-triglyceride production rate was calculated by the increase in plasma triglyceride level from baseline to 4 hours after 1 g/kg of poloxamer407 intraperitoneal injection and the data were expressed as micromoles of triglyceride produced per hour per kg of body weight. Plasma apolipoprotein

B (apoB) levels were determined by western blotting using rabbit polyclonal antibody (Abcam) in 4%-12% gradient gel (Invitrogen). The same membrane was stained with Coomassie-blue to show equal loading.

**Intraperitoneal Glucose Tolerance Test (IPGTT).** Weight-matched mice were maintained on an HFD for 6 weeks. After an overnight fast mice were weighed and received a bolus intraperitoneal injection of glucose (1 g/kg). Blood samples were obtained from a tail vein at baseline (0) and 15, 30, 45, 60, 90, and 120 minutes after glucose challenge for determination of plasma glucose and insulin concentrations.

**Reverse-Transcription Polymerase Chain Reaction (RT-PCR).** Tissue samples were obtained from mice maintained on RC or HFD for 3 months. The detailed methods, gene expression data, and sequences of PCR primers used are described in Supporting Table 2.

**Statistics.** All values are expressed as mean  $\pm$  SEM. The significance of the differences in mean values among two groups was evaluated by two-tailed unpaired Student's *t* tests. More than three groups were evaluated by analysis of variance (ANOVA) followed by post-hoc analysis using Bonferroni's Multiple Comparison Test. *P* < 0.05 was considered significant.

## Results

**APOC3 Overexpression Promotes the Development of Diet-Induced Hepatic Steatosis and NAFLD in Mice.** Increases in plasma human APOC3 were associated with significantly higher levels of plasma triglyceride in ApoC3Tg mice (Table 1). Both on RC and HFD, body weight, body composition, whole-body energy metabolism (VO<sub>2</sub>, VCO<sub>2</sub>, respiratory quotient, energy expenditure, food intake, and locomotor activity) were identical (Table 1) between WT and ApoC3Tg mice. Both groups showed identical increases in body weight and there were no differences in body composition while consuming a HFD (Table 1). Fasting plasma fatty acid concentrations were  $\approx$ 70% higher in ApoC3Tg mice, compared with WT mice (Table 1). The ApoC3Tg mice fed the HFD for  $\approx$ 3 months exhibited more severe hepatic steatosis with lipid accumulation around the Zone 3 area (Fig. 1A) than the WT, accompanied by  $\approx$ 60% increased liver triglyceride levels (Fig. 1C), which was similar between WT and ApoC3Tg mice on RC (Supporting Fig. 1). Ballooned cells, characterized by  $\approx$ 2 times the size of adjacent hepatocytes and pyknotic nucleus, were increased in ApoC3Tg mice compared with WT mice after HFD feeding (Fig. 1A). The increased liver triglyceride content in the ApoC3Tg

**Table 1. Basal Characterization for Animals**

	RC		HFD	
	WT	ApoC3Tg	WT	ApoC3Tg
Body weight (g)	29.6 ± 0.3 (n=8)	29.7 ± 0.4 (n=8)	39.5 ± 1.2† (n=8)	40.7 ± 1.1† (n=8)
Liver weight (g)	0.93 ± 0.03 (n=4)	1.0 ± 0.06 (n=4)	1.72 ± 0.12† (n=6)	2.18 ± 0.18† (n=6)
Epididymal WAT weight (g)	0.28 ± 0.05 (n=4)	0.23 ± 0.03 (n=4)	2.9 ± 0.23† (n=6)	3.1 ± 0.26† (n=6)
Body fat (%)	8.98 ± 0.9 (n=8)	9.7 ± 0.74 (n=8)	25.98 ± 1.3† (n=8)	26.31 ± 1.1† (n=8)
Lean body mass (%)	74.45 ± 0.85 (n=8)	74.29 ± 0.71 (n=8)	62.76 ± 1.43† (n=8)	63.35 ± 0.98† (n=8)
Fasting glucose (mg/dL)	118.3 ± 9.4 (n=6)	122.7 ± 11.4 (n=6)	156.4 ± 6.7† (n=8)	149.1 ± 10.9† (n=8)
Fasting insulin (μU/mL)	8.3 ± 2.0 (n=6)	11.0 ± 1.5 (n=6)	30.3 ± 6.1† (n=8)	37.3 ± 9.9† (n=8)
Fasting NEFA (mg/dL)	1.07 ± 0.11 (n=4)	1.80 ± 0.15** (n=4)	0.64 ± 0.05† (n=6)	0.97 ± 0.08*,† (n=6)
Fasting plasma triglyceride (mg/dL)	92.3 ± 6.8 (n=8)	1342 ± 221*** (n=8)	88.1 ± 14.1 (n=12)	617 ± 96.3***,† (n=12)
Human plasma APOC3 (mg/dL)	ND	209.2 ± 54.1 (n=8)	ND	106.4 ± 18.9† (n=8)
Fasting plasma adiponectin (μg/mL)	39.9 ± 3.5 (n=4)	31.4 ± 2.3 (n=4)	26.2 ± 1.9† (n=4)	31.9 ± 4.0 (n=4)
Whole body VO <sub>2</sub> [Kcal/(kg-hr)]	3077 ± 52 (n=8)	3039 ± 56 (n=8)	2775 ± 77† (n=8)	2743 ± 52† (n=8)
Whole body VCO <sub>2</sub> [Kcal/(kg-hr)]	2662 ± 60 (n=8)	2627 ± 62 (n=8)	2121 ± 57† (n=8)	2112 ± 44† (n=8)
Food intake [Kcal/(kg-hr)]	17.8 ± 1.2 (n=8)	17.5 ± 1.3 (n=8)	12.67 ± 0.52† (n=8)	13.72 ± 1.28† (n=8)
Respiratory quotient	0.86 ± 0.01 (n=8)	0.86 ± 0.01 (n=8)	0.76 ± 0.01† (n=8)	0.77 ± 0.01† (n=8)
Activity (counts)	143.6 ± 14.5 (n=8)	176 ± 25.5 (n=8)	91.0 ± 21.9 (n=8)	110.1 ± 17.4 (n=8)

WT and ApoC3Tg mice fed a RC and high fat diet for 2-3 month and fasted overnight prior to experiments.

Data are expressed as mean values ± SEM. \**P* < 0.05, \*\**P* < 0.01, \*\*\**P* < 0.001 by unpaired Student's *t* test compared to WT versus ApoC3Tg group. †*P* < 0.05 by unpaired Student's *t* test compared to RC versus HFD in each group.

ND, not detected. NEFA, nonesterified fatty acid.

mice was associated with an ≈80% increase in serum aspartate aminotransferase levels and a tendency for higher serum alanine aminotransferase levels (Fig. 1D). Fasting plasma proinflammatory cytokines were markedly increased both in WT and ApoC3Tg mice fed the HFD compared with RC fed mice and there were further increases in plasma tumor necrosis factor alpha (TNF-α) and interferon gamma (INF-γ) (both ≈70%) in ApoC3Tg mice compared with the WT mice after HFD feeding (Fig. 1E, Supporting Fig. 2). We applied a system of histological scoring designed for use in humans to systematically compare the differences in histology between the two groups. The NAFLD activity score (NAS) of ApoC3Tg mice was ≈4 (Fig. 1B) after HFD feeding, and NAS of ≥5 has been correlated with a diagnosis of NASH.<sup>15</sup> In contrast, there were no significant differences in plasma concentrations of interleukin (IL)-1β, IL-10, IL-12p70, IL-8, and IL-6 levels (Supporting Fig. 2A) or hepatic nuclear factor kappaB (NF-κB) p65, IκappaBα, or c-Jun N-terminal kinase (JNK) phosphorylation (Supporting Fig. 2A,B) between genotypes fed the HFD.

**ApoC3Tg Mice Manifest Hepatic Insulin Resistance.** In order to assess the tissue-specific contributions of liver, skeletal muscle, and adipose tissue to whole-body insulin resistance in the HFD-fed ApoC3Tg mice, we performed hyperinsulinemic-euglycemic clamp studies combined with <sup>3</sup>H/<sup>14</sup>C-labeled glucose infusions.<sup>16,17</sup> Overnight fasting plasma glucose and insulin concentrations were similar between the two groups (Table 1) as were basal rates of endogenous

glucose production (EGP) (Fig. 2E). During the hyperinsulinemic-euglycemic clamp the glucose infusion rates required to maintain euglycemia (Fig. 2A) in the ApoC3Tg mice were 34% lower than those of WT mice (Fig. 2B), indicating that the ApoC3Tg mice were more insulin resistant than the age-weight-matched WT mice. The ApoC3Tg mice displayed marked hepatic insulin resistance as reflected by the lack of suppression of EGP during the hyperinsulinemic-euglycemic clamp compared with the WT mice (Fig. 2E,F). Rates of insulin-stimulated whole-body glucose uptake were also slightly decreased by 13% in the ApoC3Tg mice compared with the WT mice (Fig. 3C), whereas muscle 2-deoxy-glucose uptake was not significantly different (Fig. 2D). Fasting plasma fatty acid concentrations decreased in a similar fashion during the hyperinsulinemic-euglycemic clamp study in both groups (% suppression: WT, 42% ± 7%; ApoC3Tg, 45% ± 6%), indicating that adipose tissue insulin responsiveness was similar between the two groups. Plasma insulin concentrations were similar between WT and ApoC3Tg mice during the clamp study (Supporting Table 1).

**ApoC3Tg Mice Have Increased Hepatic DAG Content, PKCε Activation, and Hepatic Insulin Resistance.** Increased hepatic triglyceride content and hepatic insulin resistance was associated with ≈45% increase in hepatic cytosolic DAG content in the liver from ApoC3Tg mice compared with the WT mice fed the HFD (Fig. 3A), whereas hepatic ceramide content was not different between genotypes (Supporting



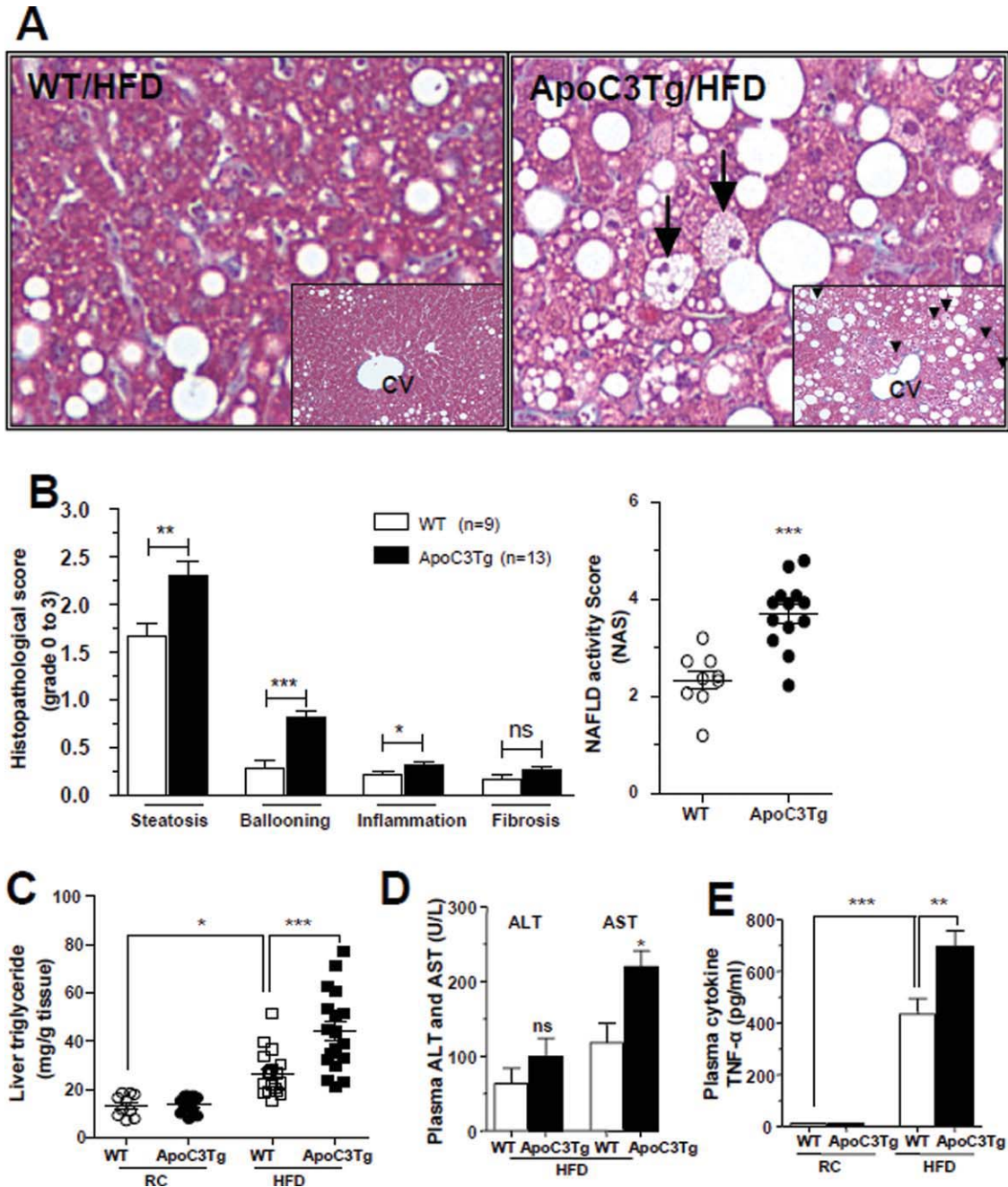


Fig. 1. APOC3 promote diet-induced hepatic steatosis and liver damage. Animals fed an RC and HFD for 2-3 months and fasted overnight prior to taking liver and blood samples. (A) Representative histological section stained with Masson-trichrome staining, examined in  $\times 400$  light microscopy field after HFD feeding for 2-3 months (insert  $\times 200$  magnifications). Arrow indicates ballooned hepatocyte. (B) Histological scoring of NAFLD in liver section after HFD feeding for 3 months. (C) Triglyceride level in the liver of WT and ApoC3Tg mice after RC and 2-3 months of HFD feeding ( $n > 10$ ). (D) Plasma ALT and AST concentration after 3 months of HFD feeding ( $n = 4$ ). (E) Plasma TNF- $\alpha$  concentration in the WT and ApoC3Tg mice after RC and 3 months of HFD feeding ( $n = 3$ , equal amounts of 4 mice plasma were pooled into each sample). Data are expressed as mean  $\pm$  SEM. \* $P < 0.05$ , \*\* $P < 0.01$ , and \*\*\* $P < 0.001$  by Student's  $t$  test for (B,D) and by ANOVA with post-hoc analysis for (C,E).

Fig. 3C,D). Furthermore, this increase in liver DAG content was associated with an  $\approx 90\%$  increase in the membrane/cytosol ratio of PKC $\epsilon$  (Fig. 3B), reflecting an increase in PKC $\epsilon$  activity, and a 32% reduction in insulin-stimulated AKT2 activity in the livers of ApoC3Tg mice compared with WT mice (Fig. 3C).

Taken together, these data are consistent with the hypothesis that increased plasma levels of APOC3 predispose animals to NAFLD and hepatic insulin resistance, which in turn can be attributed to DAG-induced PKC $\epsilon$  activation resulting in decreased insulin signaling.

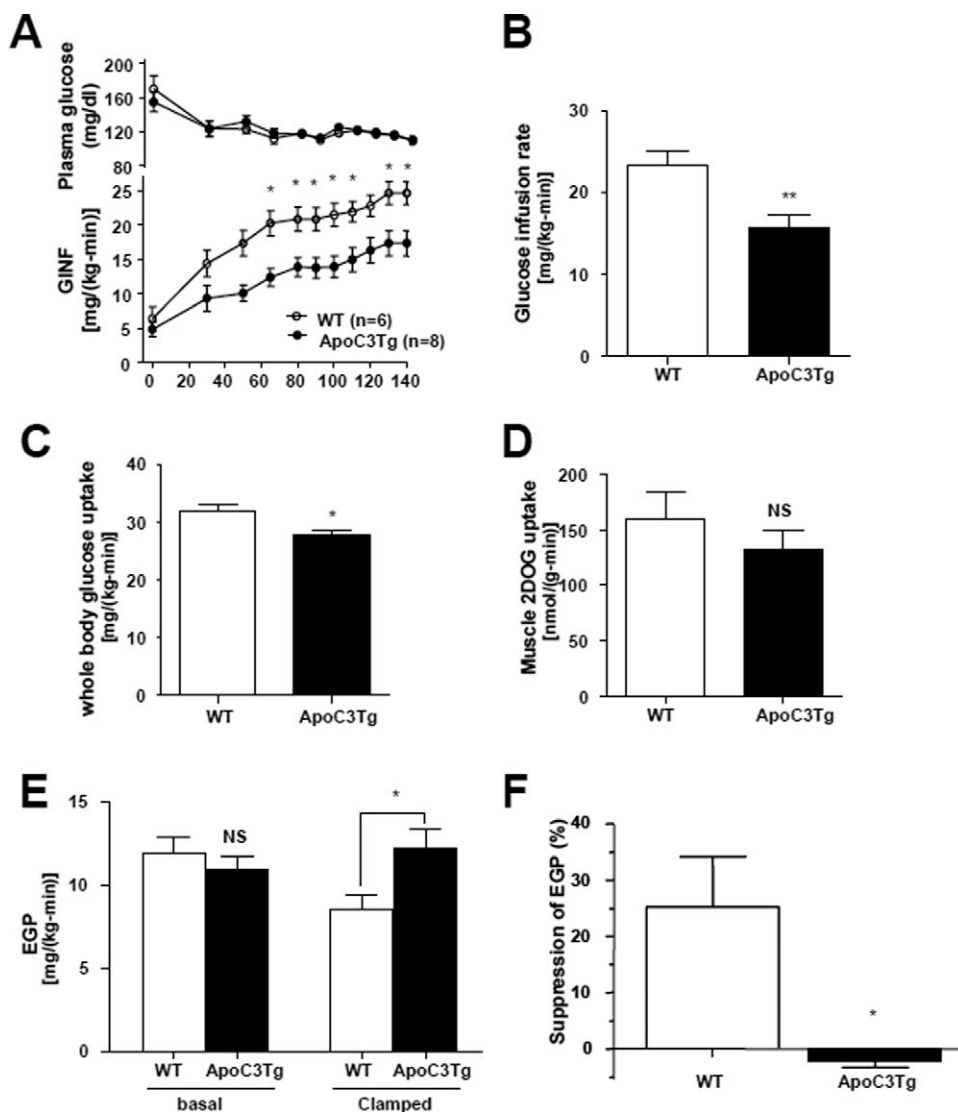


Fig. 2. Hepatic steatosis in ApoC3Tg mice is associated with hepatic insulin resistance. (A) Plasma glucose concentration and glucose infusion rate in WT ( $n = 6$ ) and ApoC3Tg ( $n = 7$ ) mice during hyperinsulinemic-euglycemic clamp study following 2 months of HFD. (B,C) Glucose infusion rate and whole-body glucose uptake rate during steady status. (D) Insulin stimulated muscle 2-deoxy-D-[ $^{14}\text{C}$ ] glucose (2DOG) uptake in gastrocnemius muscle. (E) Basal EGP and insulin suppressed (clamped) EGP and (F) percentage of suppression during the hyperinsulinemic-euglycemic clamp study. Data are expressed as mean  $\pm$  SEM. \* $P < 0.05$ , \*\* $P < 0.01$ , and \*\*\* $P < 0.001$  by Student's  $t$  test except (A) (2-way ANOVA with post-hoc analysis).

**ApoC3Tg Mice Display Increased Hepatic Triglyceride Uptake.** To address the underlying mechanism for the increased hepatic triglyceride content in the ApoC3Tg mice we assessed hepatic triglyceride uptake by intravenous injection of dual-labeled chylomicrons containing [ $^3\text{H}$ ]-retinyl ester (RE) and [ $^{14}\text{C}$ ]-triglyceride into ApoC3Tg and age-weight-matched WT littermate mice after 3 months of HFD feeding. Plasma decay of tracers in WT mice was  $0.55 \pm 0.15$  pools/min for triglyceride and  $0.19$  pools/min for RE. In ApoC3Tg mice, the plasma clearance of triglyceride was reduced to  $0.27$  pools/min, whereas that of RE was not significantly altered ( $0.17$  pools/min). These data suggest that the major effect of the APOC3 transgene was on the initial clearance of triglyceride.

We then assessed the uptake of tracer into tissues with a focus on the ratio of the two labels. The uptake

of both [ $^3\text{H}$ ]-RE-CM and [ $^{14}\text{C}$ ]-triglyceride-CM was increased by approximately twofold in the liver of ApoC3Tg mice, and the liver was the major site of TGRL uptake, compared with skeletal muscle and white adipose tissues (Fig. 4A,B). Although, in WT mice, liver triglyceride/RE uptake was  $1.00 \pm 0.05$ , indicative of greater fatty acid uptake due to lipolysis, this ratio was reduced to  $0.74 \pm 0.11$  in the ApoC3Tg mice. Triglyceride/RE uptake was  $19.4 \pm 9.67$  in skeletal muscle from WT mice, as would be expected due to greater fatty acid uptake after lipolysis. This ratio decreased to  $6.1 \pm 2.12$  in the ApoC3Tg mice. APOC3 has been reported to alter TGRL metabolism either by inhibiting lipoprotein lipase (LpL) activity or interfering with receptor-mediated hepatic uptake of remnant lipoproteins.<sup>23</sup> Our data suggest a block in peripheral triglyceride lipolysis consistent with LpL inhibition.

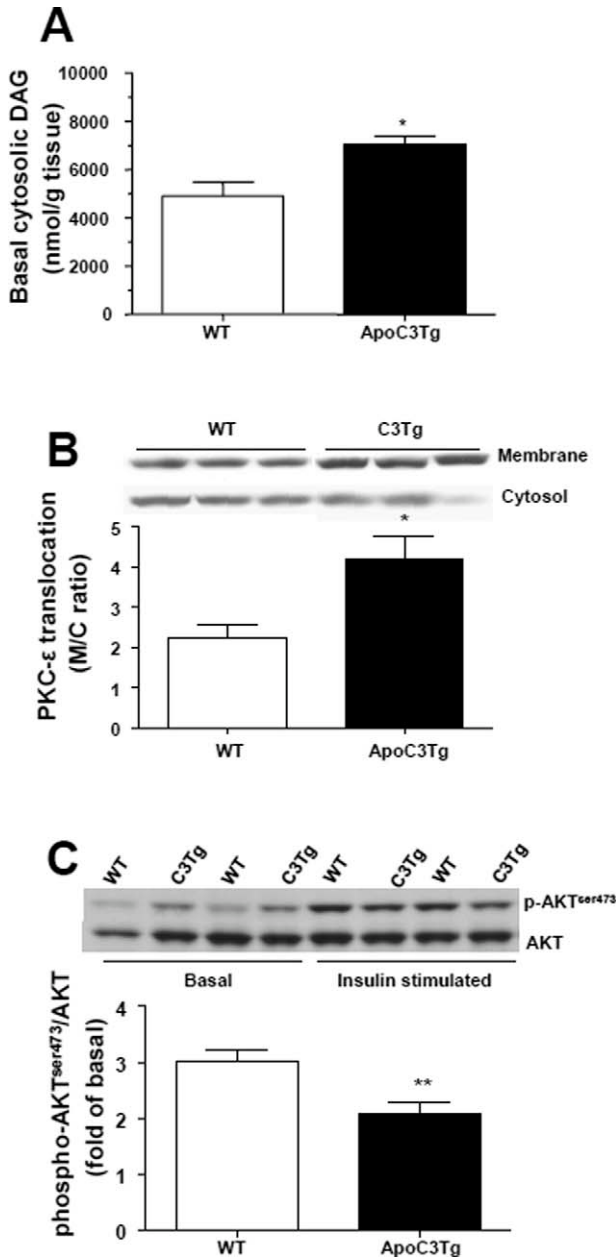


Fig. 3. Hepatic insulin resistance in the ApoC3Tg mice is associated with increased hepatic diacylglycerol content and PKC $\epsilon$  activation. Animals fed an RC and HFD for 2 months and fasted overnight prior to experiments. (A) Intracellular cytosolic diacylglycerol after overnight fasting. (B) Membrane translocation of PKC $\epsilon$  was analyzed in the liver of WT and ApoC3Tg mice after hyperinsulinemic-euglycemic clamp study. (C) Akt phosphorylation on Ser<sup>473</sup> was analyzed in the liver of overnight-fasted and hyperinsulinemic-euglycemic clamped WT and ApoC3Tg mice after 2 months of HFD feeding. Data are expressed as mean  $\pm$  SEM. (A), n = 6; (B), n = 4; (C), n = 6-7 per group. \*P < 0.05, \*\*P < 0.01 by Student's *t* test.

Because ApoC3Tg mice developed hepatic steatosis when fed an HFD diet but not when fed a regular chow diet, we also compared hepatic triglyceride uptake in ApoC3Tg and age-weight-matched WT littermates fed the RC and HFD. Surprisingly, we found

that hepatic triglyceride uptake was increased in ApoC3Tg mice fed either the RC or HFD compared with WT mice, and that there was no further increase in hepatic triglyceride uptake in the HFD-fed

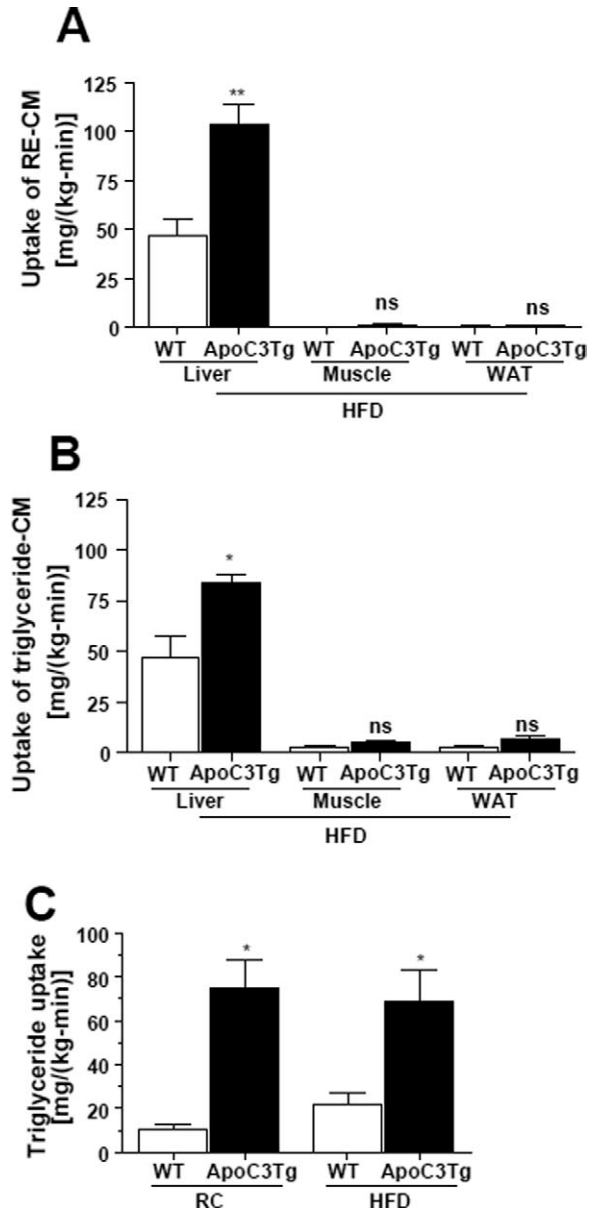


Fig. 4. Amount of hepatic triglyceride uptake was increased in ApoC3Tg mice both on RC and HFD. Animals fed an HFD for 3 months and fasted overnight prior to experiments (A,B). After collection of blood at 0 minutes, then endogenously dual-radiolabeled chylomicron,  $6 \times 10^5$  dpm of [<sup>3</sup>H]-RE-CM and  $2 \times 10^5$  dpm of [<sup>14</sup>C]-triglyceride-CM were injected. Blood was collected at 2.5, 5, 10, and 15 minutes after injection (A,B). With a separate batch of animals fed RC or HFD for 3 months, after 6 hours fasting a bolus injection of 9  $\mu$ Ci of [<sup>3</sup>H]-triolein was intravenously administered and blood samples were collected at 2.5, 5, 7.5, 10, 15, 20, 30, and 60 minutes from tail vein (C). Tissue-specific uptake rate of (A) [<sup>3</sup>H]-RE-CM (B) [<sup>14</sup>C]-triglyceride-CM were assessed in various tissues and (C) hepatic [<sup>3</sup>H]-triolein uptake rate were assessed after RC and HFD. N = 4-5. \*P < 0.05; \*\*P < 0.01; ns, not significant by Student's *t* test. CM, chylomicron. RE, retinyl ester. WAT, epididymal white adipose tissue.



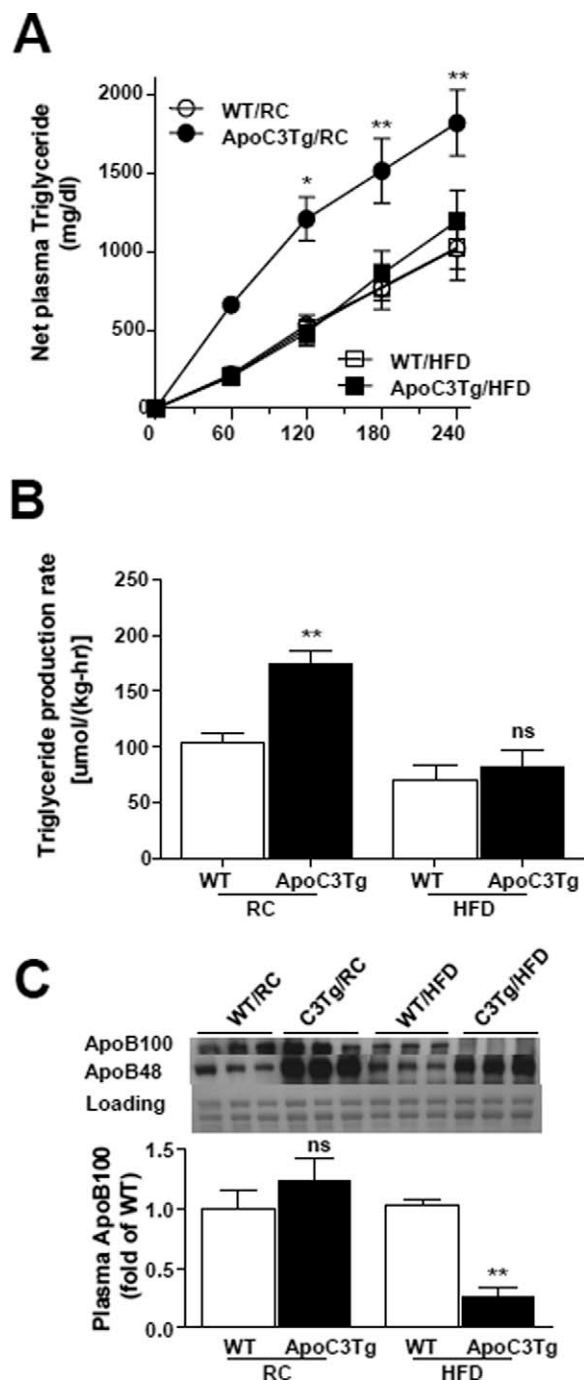


Fig. 5. Hepatic VLDL-triglyceride secretion was decreased in ApoC3Tg mice during HFD. Animals fed an RC and HFD for 3 months and fasted overnight prior to experiments. (A) Net increase of plasma triglyceride concentration after poloxamer407 (p-407) injection from basal (0 minutes, before p-407 injection) ( $n = 4-6$ ). (B) Triglyceride production rate during 4 hours after p-407 injection, expressed as micromoles of triglyceride produced per hour per kg of body weight ( $n = 4-6$ ). (C) Plasma apoB determined by western blotting using 4%-12% gradient gel. The same membrane stained with Coomassie-blue was provided as loading control ( $n = 3$ , equal amount of 4 mice plasma were pooled into each sample). Data are expressed as mean  $\pm$  SEM. \* $P < 0.05$ , \*\* $P < 0.01$ , and \*\*\* $P < 0.001$  by two-way ANOVA post-hoc analysis (A) and \*\* $P < 0.01$  by two-tailed  $t$  test (B,C). ns, not significant.

ApoC3Tg mice compared with the RC-fed ApoC3Tg mice (Fig. 4C).

**Hepatic VLDL-Triglyceride Secretion Was Decreased in ApoC3Tg Mice During HFD.** Next, we assessed VLDL-triglyceride secretion in WT and ApoC3Tg mice fed either the RC or HFD by injection of the lipoprotein lipase inhibitor poloxamer407. APOC3 has been shown to stimulate VLDL synthesis and secretion in cultured cells<sup>7</sup> and elevated circulating APOC3 levels correlate with VLDL production<sup>8</sup> and postprandial hyperlipidemia in humans.<sup>9</sup> Consistent with these findings, we observed an  $\approx 70\%$  increase in VLDL-triglyceride production in ApoC3Tg mice fed a RC diet (Fig. 5A,B), which was associated with marked increases in circulating apoB48 concentrations in ApoC3Tg mice (Fig. 5C). In contrast, we observed a 53% reduction in VLDL-triglyceride production rate in HFD-fed ApoC3Tg mice compared with the HFD-fed WT mice (Fig. 5B). The decreased VLDL-triglyceride production was accompanied by a marked decrease in circulating apoB100 level as well as a slight decrease in apoB48 concentrations in ApoC3Tg mice during HFD feeding (Fig. 5C). Liver microsomal triglyceride transfer protein (MTP) expression (Supporting Fig. 4) and messenger RNA (mRNA) expression of MTP (Supporting Table 2) were not significantly different between WT and ApoC3Tg mice on HFD. Thus, the greater uptake of TGRLs in the ApoC3Tg mice was not compensated by increased liver secretion of apoB-containing lipoproteins.

Other possible contributors to greater hepatic triglyceride content are *de novo* synthesis and reduced fatty acid oxidation. Interestingly, mRNA expression of hepatic sterol regulatory element binding protein-1c (SREBP-1c) and LpL were significantly higher in ApoC3Tg mice compared with WT on HFD (Supporting Table 2), indicating a possible contribution of increased hepatic lipogenesis to the increased hepatic lipid accumulation in ApoC3Tg mice during HFD feeding. There were no differences in whole-body oxygen consumption, respiratory quotients (Table 1), and liver mRNA expression of peroxisome proliferator-activated receptor- $\alpha$  (PPAR- $\alpha$ ) and carnitine palmitoyltransferase 1 (CPT1), between WT and ApoC3Tg mice both on RC and HFD (Supporting Table 2), suggesting that alterations in hepatic fatty acid oxidation were not likely responsible for the observed net increases in hepatic triglyceride content observed in the HFD-fed ApoC3Tg mice.

**ApoC3Tg Mice Have Reduced Hepatic ApoB100 Expression Secondary to Postprandial Hyperinsulinemia.** Recent studies have demonstrated that insulin suppresses apoB secretion in cultured hepatocytes<sup>24</sup>



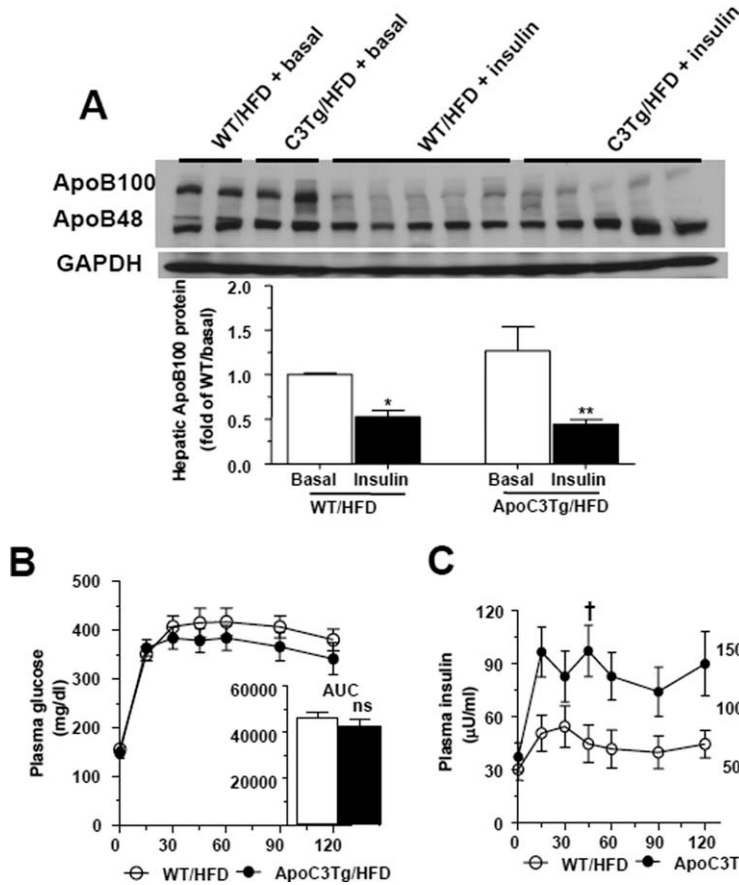


Fig. 6. Insulin suppressed hepatic apoB100 expression and postprandial insulin secretion was increased in ApoC3Tg mice after HFD feeding. (A) Hepatic apoB100 protein expression in the liver of WT and ApoC3Tg mice from overnight fasted basal and after hyperinsulinemic-euglycemic clamp study following 2 months of HFD feeding ( $n = 3$  for RC,  $n = 5$  for HFD group). (B) Plasma glucose concentration and area under curve of glucose, (C) plasma insulin level and area under curve of insulin after 1 mg/kg of glucose challenge during IPGTT in WT, and ApoC3Tg mice after 6 weeks of HFD feeding ( $n = 7$ ). Data are expressed as mean  $\pm$  SEM.  $\dagger P < 0.05$  by two-way ANOVA analysis. \* $P < 0.05$  and \*\* $P < 0.01$  by two-tailed  $t$  test. ns, not significant.

and *in vivo*.<sup>25-27</sup> In order to examine the potential role of hyperinsulinemia in causing reduced hepatic apoB100 expression in ApoC3Tg mice, we measured hepatic apoB100 protein levels in HFD-fed ApoC3Tg and WT mice at the end of the hyperinsulinemic-euglycemic clamp and found that insulin rapidly suppressed hepatic apoB100 expression both in the liver of WT and ApoC3Tg mice (Fig. 6A). We next examined whether ApoC3Tg mice exhibited increased plasma insulin concentrations following an intraperitoneal glucose tolerance test. Plasma glucose concentrations were similar between HFD-fed WT and ApoC3Tg mice after glucose challenge (Fig. 5B). In contrast, ApoC3Tg mice had an  $\approx 120\%$  increase in peak and an  $\approx 70\%$  increase in the AUC of glucose-stimulated plasma insulin concentrations compared with WT mice (Fig. 5C), reflecting whole-body insulin resistance as well as increased postprandial insulin secretion in ApoC3Tg mice on HFD. Taken together, these data suggest that the increase in net hepatic triglyceride content in the HFD-fed ApoC3Tg mice can likely be attributed to both an increase in hepatic triglyceride uptake in combination with decreased hepatic VLDL secretion, due to suppression

of hepatic apoB expression from chronic postprandial hyperinsulinemia.

## Discussion

Previous studies have found that whole-body insulin-mediated glucose disposal was unchanged without any ectopic lipid deposition in ApoC3Tg mice fed an RC diet.<sup>6,28</sup> In contrast to these findings, we found that when ApoC3Tg mice were challenged with an HFD they developed NASH associated with marked hepatic insulin resistance compared with WT littermate mice fed the same diet. These data provide important genetic verification of a recent study showing that healthy lean individuals carrying variants in the insulin response element of the APOC3 gene, leading to increased APOC3 concentrations in plasma, are predisposed to developing NAFLD associated with insulin resistance.<sup>9</sup>

Interestingly, we found that ApoC3Tg mice were more prone to develop hepatic steatohepatitis as reflected by the histologic NAFLD score and increased serum aspartate aminotransferase (AST), TNF- $\alpha$ , and INF- $\gamma$  concentrations. These data are consistent with

previous data demonstrating that APOC3 can cause inflammation in various cells, including endothelial cells,<sup>10</sup> monocytes,<sup>29</sup> and adipose tissue,<sup>11</sup> and support the hypothesis that increased plasma levels of APOC3 may also make individuals more prone to develop NASH in addition to simple steatosis.<sup>9</sup> However, the increased circulating cytokines were not associated with hepatic NF- $\kappa$ B p65, JNK phosphorylation, and ceramide content, indicating the hepatic inflammatory signals may not be the major factors for aggravating the hepatic insulin resistance in ApoC3Tg mice. In contrast, we found that the NAFLD and hepatic insulin resistance could be attributed to increased hepatocellular DAG content and activation of PKC $\epsilon$ , which we have previously demonstrated causes decreased insulin signaling at the level of the insulin receptor kinase.<sup>20,30</sup> This finding is in contrast to another recent report of a PNPLA gene variant that was associated with NAFLD but was not associated with insulin resistance.<sup>31</sup>

Furthermore, we found that hepatic triglyceride uptake was surprisingly increased in ApoC3Tg mice fed either the RC or HFD despite the absence of hepatic steatosis when the ApoC3Tg mice were fed the RC diet. We went on to show that ApoC3Tg mice fed the HFD have reduced hepatic VLDL production, which could be attributed to decreased hepatic apoB100 expression from chronic hyperinsulinemia. Taken together, these findings suggest that increased hepatic expression of APOC3 promotes increased hepatic triglyceride uptake that is compensated for by increased hepatic VLDL production in ApoC3Tg mice fed RC. In contrast, ApoC3Tg mice fed an HFD are unable to compensate with increased VLDL production due to postprandial hyperinsulinemia, leading to suppression of hepatic apoB100 and VLDL production and to net hepatic triglyceride accumulation. In addition, we also found an  $\approx$ 6-fold and  $\approx$ 2-fold increase in expression of LpL and SREBP1c mRNA, respectively, in the livers of the ApoC3Tg mice following HFD, which may also have contributed to the development of hepatic steatosis in these mice. These findings may also explain the mechanism of hepatic lipid accumulation in the other mouse models of hepatic steatosis and steatohepatitis that showed severe hyperlipidemia such as apolipoprotein E (APOE)-deficient mice and LDL receptor-deficient mice.<sup>32-34</sup>

Many of the postulated effects of APOC3 on peripheral and tissue lipid metabolism were confirmed in our studies. As had been reported,<sup>6,35</sup> using endogenously labeled chylomicrons we confirmed that one reason for the hypertriglyceridemia in these animals is

reduced plasma clearance. *In vitro* studies by these investigators found that VLDL from the APOC3 transgenic mice were lipolyzed normally by LpL but had reduced uptake into cells<sup>6</sup>; this latter finding is what one would expect from nonlipolyzed TGRLs that interact poorly with lipoprotein receptors. Our data showing that skeletal muscle uptake of triglyceride is much more impaired than its uptake of RE is more consistent with APOC3 functioning as an inhibitor of lipolysis. In addition, the observations that APOC3 overexpression leads to hypertriglyceridemia in APOE knockout mice<sup>36</sup> and causes less hypertriglyceridemia in apoB48 only mice that are more dependent on non-LDL receptor-mediated lipid uptake<sup>37</sup> are consistent with LpL inhibition.

In summary, we found that transgenic mice with hepatic overexpression of human APOC3 were more prone to develop hepatic steatosis associated with hepatic insulin resistance compared with WT littermates fed the same HFD diet. This study provides strong genetic evidence in support of the hypothesis that increased plasma APOC3 concentrations predispose lean individuals to NAFLD associated with hepatic insulin resistance.<sup>9</sup> Importantly, the development of NAFLD associated with hepatic insulin resistance in response to dietary alterations exemplifies how gene-environment interactions contribute to the pathogenesis of complex phenotypes.

*Acknowledgment:* We thank to Irena Ignatova-Todorova, Xiaoxian Ma, Mario Kahn, Christopher M. Carmean for expert technical assistance with the studies and Dr. Jan Breslow (Rockefeller University, New York, NY) for providing the ApoC3Tg mice.

## References

- Petersen KF, Oral EA, Dufour S, Befroy D, Ariyan C, Yu C, et al. Leptin reverses insulin resistance and hepatic steatosis in patients with severe lipodystrophy. *J Clin Invest* 2002;109:1345-1350.
- Seppala-Lindroos A, Vehkavaara S, Hakkinen AM, Goto T, Westerbacka J, Sovijarvi A, et al. Fat accumulation in the liver is associated with defects in insulin suppression of glucose production and serum free fatty acids independent of obesity in normal men. *J Clin Endocrinol Metab* 2002;87:3023-3028.
- Petersen KF, Dufour S, Befroy D, Lehrke M, Hendler RE, Shulman GI. Reversal of nonalcoholic hepatic steatosis, hepatic insulin resistance, and hyperglycemia by moderate weight reduction in patients with type 2 diabetes. *Diabetes* 2005;54:603-608.
- Ito Y, Azrolan N, O'Connell A, Walsh A, Breslow JL. Hypertriglyceridemia as a result of human apo CIII gene expression in transgenic mice. *Science* 1990;249:790-793.
- Pollin TI, Damcott CM, Shen H, Ott SH, Shelton J, Horenstein RB, et al. A null mutation in human APOC3 confers a favorable plasma lipid profile and apparent cardioprotection. *Science* 2008;322:1702-1705.
- Aalto-Setälä K, Fisher EA, Chen X, Chajek-Shaul T, Hayek T, Zechner R, et al. Mechanism of hypertriglyceridemia in human apolipoprotein

- (apo) CIII transgenic mice. Diminished very low density lipoprotein fractional catabolic rate associated with increased apo CIII and reduced apo E on the particles. *J Clin Invest* 1992;90:1889-1900.
7. Sundaram M, Zhong S, Bou Khalil M, Links PH, Zhao Y, Iqbal J, et al. Expression of apolipoprotein C-III in McA-RH7777 cells enhances VLDL assembly and secretion under lipid-rich conditions. *J Lipid Res* 2010;51:150-161.
  8. Cohn JS, Patterson BW, Uffelman KD, Davignon J, Steiner G. Rate of production of plasma and very-low-density lipoprotein (VLDL) apolipoprotein C-III is strongly related to the concentration and level of production of VLDL triglyceride in male subjects with different body weights and levels of insulin sensitivity. *J Clin Endocrinol Metab* 2004;89:3949-3955.
  9. Petersen KF, Dufour S, Hariri A, Nelson-Williams C, Foo JN, Zhang XM, et al. Apolipoprotein C3 gene variants in nonalcoholic fatty liver disease. *N Engl J Med* 2010;362:1082-1089.
  10. Kawakami A, Aikawa M, Alcaide P, Lusinskas FW, Libby P, Sacks FM. Apolipoprotein CIII induces expression of vascular cell adhesion molecule-1 in vascular endothelial cells and increases adhesion of monocytic cells. *Circulation* 2006;114:681-687.
  11. Abe Y, Kawakami A, Osaka M, Uematsu S, Akira S, Shimokado K, et al. Apolipoprotein CIII induces monocyte chemoattractant protein-1 and interleukin 6 expression via Toll-like receptor 2 pathway in mouse adipocytes. *Arterioscler Thromb Vasc Biol* 2010;30:2242-2248.
  12. Pollex RL, Ban MR, Young TK, Bjerregaard P, Anand SS, Yusuf S, et al. Association between the -455T>C promoter polymorphism of the APOC3 gene and the metabolic syndrome in a multi-ethnic sample. *BMC Med Genet* 2007;8:80.
  13. Waterworth DM, Ribalta J, Nicaud V, Dallongeville J, Humphries SE, Talmud P. ApoCIII gene variants modulate postprandial response to both glucose and fat tolerance tests. *Circulation* 1999;99:1872-1877.
  14. Lee HY, Park JH, Seok SH, Baek MW, Kim DJ, Lee KE, et al. Human originated bacteria, *Lactobacillus rhamnosus* PL60, produce conjugated linoleic acid and show anti-obesity effects in diet-induced obese mice. *Biochim Biophys Acta* 2006;1761:736-744.
  15. Kleiner DE, Brunt EM, Van Natta M, Behling C, Contos MJ, Cummings OW, et al. Design and validation of a histological scoring system for nonalcoholic fatty liver disease. *HEPATOLOGY* 2005;41:1313-1321.
  16. Lee HY, Choi CS, Birkenfeld AL, Alves TC, Jornayvaz FR, Jurczak MJ, et al. Targeted expression of catalase to mitochondria prevents age-associated reductions in mitochondrial function and insulin resistance. *Cell Metab* 2010;12:668-674.
  17. Samuel VT, Choi CS, Phillips TG, Romanelli AJ, Geisler JG, Bhanot S, et al. Targeting foxo1 in mice using antisense oligonucleotide improves hepatic and peripheral insulin action. *Diabetes* 2006;55:2042-2050.
  18. Bligh EG, Dyer WJ. A rapid method of total lipid extraction and purification. *Can J Biochem Physiol* 1959;37:911-917.
  19. Yu C, Chen Y, Cline GW, Zhang D, Zong H, Wang Y, et al. Mechanism by which fatty acids inhibit insulin activation of insulin receptor substrate-1 (IRS-1)-associated phosphatidylinositol 3-kinase activity in muscle. *J Biol Chem* 2002;277:50230-50236.
  20. Samuel VT, Liu ZX, Qu X, Elder BD, Bilz S, Befroy D, et al. Mechanism of hepatic insulin resistance in non-alcoholic fatty liver disease. *J Biol Chem* 2004;279:32345-32353.
  21. Choi CS, Fillmore JJ, Kim JK, Liu ZX, Kim S, Collier EF, et al. Overexpression of uncoupling protein 3 in skeletal muscle protects against fat-induced insulin resistance. *J Clin Invest* 2007;117:1995-2003.
  22. Bharadwaj KG, Hiyama Y, Hu Y, Huggins LA, Ramakrishnan R, Abumrad NA, et al. Chylomicron- and VLDL-derived lipids enter the heart through different pathways: in vivo evidence for receptor- and non-receptor-mediated fatty acid uptake. *J Biol Chem* 2010;285:37976-37986.
  23. Ginsberg HN, Brown WV. Apolipoprotein CIII: 42 years old and even more interesting. *Arterioscler Thromb Vasc Biol* 2011;31:471-473.
  24. Salhanick AI, Schwartz SI, Amatruda JM. Insulin inhibits apolipoprotein B secretion in isolated human hepatocytes. *Metabolism* 1991;40:275-279.
  25. Sparks JD, Sparks CE. Insulin regulation of triacylglycerol-rich lipoprotein synthesis and secretion. *Biochim Biophys Acta* 1994;1215:9-32.
  26. Lewis GF, Steiner G. Acute effects of insulin in the control of VLDL production in humans. Implications for the insulin-resistant state. *Diabetes Care* 1996;19:390-393.
  27. Sorensen LP, Andersen IR, Sondergaard E, Gormsen LC, Schmitz O, Christiansen JS, et al. Basal and insulin mediated VLDL-triglyceride kinetics in type 2 diabetic men. *Diabetes* 2011;60:88-96.
  28. Reaven GM, Mondon CE, Chen YD, Breslow JL. Hypertriglyceridemic mice transgenic for the human apolipoprotein C-III gene are neither insulin resistant nor hyperinsulinemic. *J Lipid Res* 1994;35:820-824.
  29. Kawakami A, Osaka M, Aikawa M, Uematsu S, Akira S, Libby P, et al. Toll-like receptor 2 mediates apolipoprotein CIII-induced monocyte activation. *Circ Res* 2008;103:1402-1409.
  30. Samuel VT, Liu ZX, Wang A, Beddow SA, Geisler JG, Kahn M, et al. Inhibition of protein kinase Cepsilon prevents hepatic insulin resistance in nonalcoholic fatty liver disease. *J Clin Invest* 2007;117:739-745.
  31. Romeo S, Kozlitina J, Xing C, Pertsemlidis A, Cox D, Pennacchio LA, et al. Genetic variation in PNPLA3 confers susceptibility to nonalcoholic fatty liver disease. *Nat Genet* 2008;40:1461-1465.
  32. Rull A, Escola-Gil JC, Julve J, Rotllan N, Calpe-Berdiel L, Coll B, et al. Deficiency in monocyte chemoattractant protein-1 modifies lipid and glucose metabolism. *Exp Mol Pathol* 2007;83:361-366.
  33. Rull A, Rodriguez F, Aragones G, Marsillach J, Beltran R, Alonso-Villaverde C, et al. Hepatic monocyte chemoattractant protein-1 is upregulated by dietary cholesterol and contributes to liver steatosis. *Cytokine* 2009;48:273-279.
  34. Lohmann C, Schafer N, von Lukowicz T, Sokrates Stein MA, Boren J, Rutti S, et al. Atherosclerotic mice exhibit systemic inflammation in periaortic and visceral adipose tissue, liver, and pancreatic islets. *Atherosclerosis* 2009;207:360-367.
  35. de Silva HV, Lauer SJ, Wang J, Simonet WS, Weisgraber KH, Mahley RW, et al. Overexpression of human apolipoprotein C-III in transgenic mice results in an accumulation of apolipoprotein B48 remnants that is corrected by excess apolipoprotein E. *J Biol Chem* 1994;269:2324-2335.
  36. Ebara T, Ramakrishnan R, Steiner G, Shachter NS. Chylomicronemia due to apolipoprotein CIII overexpression in apolipoprotein E-null mice. Apolipoprotein CIII-induced hypertriglyceridemia is not mediated by effects on apolipoprotein E. *J Clin Invest* 1997;99:2672-2681.
  37. Conde-Knape K, Okada K, Ramakrishnan R, Shachter NS. Overexpression of apoC-III produces lesser hypertriglyceridemia in apoB-48-only gene-targeted mice than in apoB-100-only mice. *J Lipid Res* 2004;45:2235-2244.